

# CP violation Beyond the MSSM: Baryogenesis and Electric Dipole Moments

Kfir Blum,<sup>1</sup> Cedric Delaunay,<sup>1</sup> Marta Losada,<sup>2</sup> Yosef Nir,<sup>1</sup> and Sean Tulin<sup>3</sup>

<sup>1</sup>*Department of Particle Physics and Astrophysics,  
Weizmann Institute of Science, Rehovot 76100, Israel*

<sup>2</sup>*Centro de Investigaciones, Cra 3 Este No 47A-15,  
Universidad Antonio Nariño, Bogotá, Colombia*

<sup>3</sup>*Theory Group, TRIUMF, 4004 Wesbrook Mall,  
Vancouver, BC, V6T 2A3, Canada*

(Dated: August 15, 2021)

## Abstract

We study electroweak baryogenesis and electric dipole moments in the presence of the two leading-order, non-renormalizable operators in the Higgs sector of the MSSM. Significant qualitative and quantitative differences from MSSM baryogenesis arise due to the presence of new CP-violating phases and to the relaxation of constraints on the supersymmetric spectrum (in particular, both stops can be light). We find: (1) spontaneous baryogenesis, driven by a change in the phase of the Higgs vevs across the bubble wall, becomes possible; (2) the top and stop CP-violating sources can become effective; (3) baryogenesis is viable in larger parts of parameter space, alleviating the well-known fine-tuning associated with MSSM baryogenesis. Nevertheless, electric dipole moments should be measured if experimental sensitivities are improved by about one order of magnitude.

## I. INTRODUCTION

Electroweak baryogenesis (EWBG) is an attractive mechanism for generating the baryon asymmetry of the Universe (BAU). Its primary attraction is the possibility to experimentally test two of the three Sakharov conditions. Aspects of the departure from thermal equilibrium via the electroweak phase transition (EWPT) can be explored in collider experiments, while CP violation can be tested in electric dipole moment (EDM) searches.

In the EWBG picture, electroweak symmetry breaking proceeds via a first-order phase transition, where bubbles of broken  $SU(2)_L$  symmetry nucleate and expand in a background of unbroken symmetry. CP-violating interactions within the bubble walls lead to the production of CP-asymmetric charge density of left-handed fermions. This charge, diffusing ahead of the wall into the unbroken phase, is converted into the BAU by non-perturbative, electroweak sphaleron processes. To the extent that electroweak sphalerons are inactive after electroweak symmetry breaking, the baryon density “freezes out” once it is captured by the advancing bubble wall. This mechanism satisfies the Sakharov criteria [1] and generates the BAU provided two conditions are met: (1) the phase transition is “strongly” first-order (otherwise electroweak sphalerons are active within the broken phase and washout the BAU), and (2) the CP violation is sufficient to generate the observed BAU. Neither of these conditions are met in the Standard Model (SM) [2].

Beyond the SM, the most widely studied EWBG model has been the Minimal Supersymmetric Standard Model (MSSM). However, there are a series of tensions that make this scenario severely constrained by experiment. First, there is tension in the top squark (“stop”) sector. A strong first-order phase transition requires at least one light stop (which must be mostly  $\tilde{t}_R$ , to avoid large contributions to the  $\rho$  parameter and due to null searches for a light sbottom [3, 4]). At the same time, the large radiative corrections needed to push the Higgs boson mass above the LEP bound  $m_h > 114$  GeV [4] require that at least one stop ( $\tilde{t}_L$ ) is very heavy [5]. Recently, the phase transition was studied in an effective theory with a large stop hierarchy, concluding that successful EWBG is possible only for  $m_{\tilde{t}_R} < 125$  GeV and  $m_{\tilde{t}_L} > 6.5$  TeV [6], rendering the scenario finely tuned.

Second, there is tension between having enough CP violation to produce the BAU and evading stringent constraints from EDM searches. In the MSSM, the CP-violating phases that drive EWBG arise in the gaugino/higgsino sector. The same phases contribute to

EDMs. While one-loop contributions can be sufficiently suppressed by making the first two squark and slepton generations heavy, there exist two-loop contributions that cannot be suppressed without spoiling EWBG (assuming no fine-tuned cancellation between different EDM contributions) and which predict a minimum value of the EDM. These “irreducible” EDMs strongly constrain the viable MSSM parameter space: EWBG with universal gaugino phases is nearly ruled out. With improvements by a factor 3–4 in the upper bounds on the EDMs of the electron or the neutron, MSSM baryogenesis will be possible only in the so-called “bino-driven” scenario, where the CP-violating phase associated with the  $U(1)_Y$  gaugino is tuned to be much larger than that of the  $SU(2)_L$  gaugino [7, 8].

Third, there is tension in the mass of the pseudoscalar Higgs boson  $A_0$ . Large values of  $m_A$  are preferred (i) to make the EWPT more strongly first-order, and (ii) to evade constraints from  $b \rightarrow s\gamma$  [8]. However, the production of left-handed charge during EWBG is enhanced when  $m_A$  is light. There is also a tension in the value of  $\tan\beta$  (i) from a compromise in giving a large enough value of the Higgs mass versus a strong enough phase transition, and (ii) from the constraints from  $b \rightarrow s\gamma$  for small values of  $m_A$ . All in all, from the theoretical point of view, these tensions force the MSSM (if it is to account for EWBG) into a narrow, finely tuned region of parameter space.

An attractive extension of the MSSM is the “Beyond the MSSM” (BMSSM) scenario [9]. Here, a non-renormalizable contribution to the MSSM superpotential is included

$$W_{\text{BMSSM}} = W_{\text{MSSM}} + \frac{\lambda}{M} (H_u H_d)^2, \quad (1)$$

as well as a contribution to the soft SUSY-breaking Lagrangian

$$\mathcal{L}_{\text{soft}}^{\text{BMSSM}} = \mathcal{L}_{\text{soft}}^{\text{MSSM}} + \frac{\lambda_s m_{\text{SUSY}}}{M} (H_u H_d)^2, \quad (2)$$

encoding the leading supersymmetric and  $F$ -term supersymmetry breaking corrections to the Higgs sector that arise from a new threshold at mass scale  $M$  [10–14]. The corrections enter the spectrum and interactions through the dimensionless parameters

$$\epsilon_1 \equiv \frac{\lambda \mu^*}{M}, \quad \epsilon_2 \equiv -\frac{\lambda_s m_{\text{SUSY}}}{M}. \quad (3)$$

For  $M \sim \text{few TeV}$ , the BMSSM has interesting implications for cosmology [15–19] and for Higgs phenomenology [20]. The BMSSM operators, which contribute at tree-level to the

MSSM phases		BMSSM phases		vev phase
$\phi_i$	$\phi_f$	$\vartheta_1$	$\vartheta_2$	$\theta$
$\arg(M_i\mu/b)$	$\arg(A_f\mu/b)$	$\arg(\epsilon_1/b)$	$\arg(\epsilon_2/b^2)$	$\arg(b H_u H_d)$

TABLE I: *The CP-violating phases in the BMSSM. Here  $i = 1, 2, 3$  labels gaugino mass parameters and  $f$  labels the trilinear sfermion-Higgs coupling corresponding to a SM fermion  $f$ .*

Higgs mass, alleviate the tension associated with the stop sector and  $\tan\beta$ . Now, the left-handed stop can also be relatively light, providing additional bosonic degrees of freedom that strengthen the first-order phase transition<sup>1</sup>.

In this work, we examine the BMSSM implications for CP violation and the generation of the baryon asymmetry. In Sec. II, we describe new CP-violating phases associated with the BMSSM operators. In Sec. III, we review relevant aspects of the phase transition dynamics and show that these phases lead to new CP-violating sources that generate charge density during the phase transition. In this section we also compute the resulting BAU. In Sec. IV, we discuss how searches for EDMs constrain CP violation and baryogenesis in the BMSSM. We conclude in Sec. V. The appendices contain details of the CP-violating vacuum structure and radiative corrections to the Higgs CP-violating phase.

## II. CP VIOLATION

In this section, we describe the BMSSM Lagrangian to leading order in  $M^{-1}$ , emphasizing those aspects that are relevant for CP violation, baryogenesis, and EDMs. The new BMSSM phases (denoted  $\vartheta_{1,2}$ ) lead to (i) explicit CP violation in the neutralino, chargino, and squark mass matrices, and (ii) CP-violating mixing of the Higgs pseudoscalar  $A_0$  with the two other neutral Higgs scalars  $h_0, H_0$ . We express our results in terms of physical CP-violating phases that are invariant under phase redefinitions of fields, summarized in Table I.

Neglecting flavor mixing, the invariant phases of Table I provide a complete basis for all of the rephasing invariants in the BMSSM. Such basis is easily constructed by noting that Higgs field rephasing is equivalent to global  $U(1)_{PQ}$  and  $U(1)_{R-PQ}$  transformations [22].

---

<sup>1</sup> To be clear, a first-order phase transition is induced radiatively through thermal effects, similar to the MSSM, as opposed to new tree-level interactions as in, *e.g.*, the NMSSM [21].

The  $U(1)_{PQ}$  and  $U(1)_{R-PQ}$  are explicitly broken by the dimensionful MSSM parameters appearing in Table I, as well as by the BMSSM new effective couplings. By promoting the parameters to spurions with well-defined transformation properties, one can extract the rephasing invariants in terms of  $U(1)_{PQ}$  and  $U(1)_{R-PQ}$  conserving combinations.

We follow the notation of Ref. [23] with respect to the MSSM parameters. In our numerical analysis we implement the quantum corrections from the neutralino, chargino, scalar Higgs, and squark sectors. Details are given in Appendix B. CP violation induced by these corrections in the Higgs sector is suppressed for small values of the trilinear  $A$  term and for moderate values of  $\mu$ , which we adopt throughout our analysis. This allows us to focus on the novel tree-level BMSSM effects.

First, we consider the tree-level Higgs potential

$$V_0 = (m_{H_u}^2 + |\mu|^2) |H_u|^2 + (m_{H_d}^2 + |\mu|^2) |H_d|^2 + \frac{g'^2 + g^2}{8} (|H_u|^2 - |H_d|^2)^2 + \frac{g^2}{2} |H_d^\dagger H_u|^2 + \left( b (H_u H_d) + 2 \epsilon_1 (|H_u|^2 + |H_d|^2) (H_u H_d) + \epsilon_2 (H_u H_d)^2 + \text{h.c.} \right), \quad (4)$$

with  $SU(2)_L$  contractions defined as  $(H_u H_d) \equiv H_u^+ H_d^- - H_u^0 H_d^0$ . At zero temperature, the Higgs vacuum expectation values (vevs) are

$$\langle H_u^0 \rangle \equiv v_u = s_\beta v e^{i\theta_u}, \quad \langle H_d^0 \rangle \equiv v_d = c_\beta v e^{i\theta_d} \quad (5)$$

where  $\tan \beta \equiv |v_u/v_d|$ ,  $s_\beta \equiv \sin \beta$ ,  $c_\beta \equiv \cos \beta$ , and  $v \simeq 174$  GeV. The relative phase  $(\theta_u - \theta_d)$  is unphysical and can be set to zero by a gauge transformation. We define the Higgs phase  $\theta$  as

$$\theta_u + \theta_d \equiv \theta - \arg(b). \quad (6)$$

It is useful to factor out  $\arg(b)$  explicitly, since  $\theta$  is rephasing invariant [24]<sup>2</sup>. Next, we define rephasing invariant BMSSM parameters

$$\epsilon_{1r} \equiv |\epsilon_1| \cos(\vartheta_1 + \theta) \quad \epsilon_{1i} \equiv |\epsilon_1| \sin(\vartheta_1 + \theta) \quad (7a)$$

$$\epsilon_{2r} \equiv |\epsilon_2| \cos(\vartheta_2 + 2\theta) \quad \epsilon_{2i} \equiv |\epsilon_2| \sin(\vartheta_2 + 2\theta). \quad (7b)$$

---

<sup>2</sup> In Ref. [25], explicit CP violation in the BMSSM was also studied. However, the authors considered a scenario in which  $\arg(b) = \theta_u + \theta_d = 0$ . Since  $\theta$  is rephasing invariant, Ref. [25] deals with a very specific physical model, and the results derived there do not apply in general.

In the phase convention  $\theta_u + \theta_d = 0$ , our definitions reduce to the usual definitions  $\epsilon_{1r} = \text{Re}[\epsilon_1]$ , *etc.* [9].

The masses and mixing angles of the physical Higgs bosons receive tree-level corrections from the BMSSM operators. In our expressions to follow, we work at tree-level and eliminate the set of parameters  $(m_{H_u}^2, m_{H_d}^2, |b|)$  in favor of  $(v, \tan \beta, m_A)$ . We parametrize the Higgs fields in the following way:

$$H_u = e^{i\theta_u} \begin{pmatrix} H_u^+ \\ s_\beta v + \frac{h_u + i a_u}{\sqrt{2}} \end{pmatrix}, \quad H_d = e^{i\theta_d} \begin{pmatrix} c_\beta v + \frac{h_d + i a_d}{\sqrt{2}} \\ H_d^- \end{pmatrix}. \quad (8)$$

In the limit  $\epsilon_{1i} = \epsilon_{2i} = 0$ , one can separately diagonalize the CP-even and odd Higgs states, as in the MSSM [23]. The eigenstates are

$$\begin{pmatrix} h_0 \\ H_0 \end{pmatrix} = \begin{pmatrix} \cos \alpha & -\sin \alpha \\ \sin \alpha & \cos \alpha \end{pmatrix} \begin{pmatrix} h_u \\ h_d \end{pmatrix}, \quad \begin{pmatrix} G_0 \\ A_0 \end{pmatrix} = \begin{pmatrix} \sin \beta & -\cos \beta \\ \cos \beta & \sin \beta \end{pmatrix} \begin{pmatrix} a_u \\ a_d \end{pmatrix}, \quad (9)$$

with Higgs mixing angle  $\alpha$  given by

$$\cos 2\alpha = -\frac{m_A^2 - m_Z^2 + 4\epsilon_{2r}v^2}{m_H^2 - m_h^2} \cos 2\beta, \quad \sin 2\alpha = -\frac{(m_A^2 + m_Z^2) \sin 2\beta - 8\epsilon_{1r}v^2}{m_H^2 - m_h^2}. \quad (10)$$

The mass eigenvalues also receive tree-level contributions proportional to  $\epsilon_{1,2r}$  [9]. In particular, the lightest Higgs boson receives a correction

$$\delta_\epsilon m_h^2 = 2v^2 \left( \epsilon_{2r} - 2\epsilon_{1r}s_{2\beta} - \frac{2\epsilon_{1r}(m_A^2 + m_Z^2)s_{2\beta} + \epsilon_{2r}(m_A^2 - m_Z^2)c_{2\beta}^2}{\sqrt{(m_A^2 - m_Z^2)^2 + 4m_A^2 m_Z^2 s_{2\beta}^2}} \right). \quad (11)$$

This contribution can increase the tree-level Higgs mass above the LEP bound, without the need for radiative corrections [26]. It is important to recall that the LEP bound on the lightest neutral Higgs boson mass is drastically changed in the presence of CP violation [27]. In fact, there are allowed regions even for very small values of the Higgs boson mass. In principle this implies that a much larger region in parameter space can accommodate a strong first order phase transition and the right-handed stop can be heavier than the top quark. However, as we will see below, there are significant constraints on the amount of CP violation.

CP violation enters the Higgs sector at tree-level when  $\epsilon_{1,2i} \neq 0$ , leading to mixing between

CP eigenstates. In the  $(h_0, H_0, A_0)$  basis, the Higgs mass matrix is

$$M_{H_0}^2 = \begin{pmatrix} m_h^2 & 0 & m_{hA}^2 \\ 0 & m_H^2 & m_{HA}^2 \\ m_{hA}^2 & m_{HA}^2 & m_A^2 \end{pmatrix}. \quad (12)$$

The remaining CP-odd state  $G_0$  is eaten by the  $Z$  boson. The parameters  $m_{hA}^2$  and  $m_{HA}^2$ , which govern the mixing between CP-even and odd states, are given by

$$m_{hA}^2 = 4v^2 \epsilon_{1i} \sin(\beta - \alpha) - 2v^2 \epsilon_{2i} \cos(\alpha + \beta) \approx -2v^2 (\epsilon_{2i} s_{2\beta} - 2\epsilon_{1i}), \quad (13)$$

$$m_{HA}^2 = 4v^2 \epsilon_{1i} \cos(\beta - \alpha) - 2v^2 \epsilon_{2i} \sin(\alpha + \beta) \approx 2v^2 \epsilon_{2i} c_{2\beta}, \quad (14)$$

where the approximations follow in the limit of moderate  $\tan \beta$  and  $m_A^2 \gg m_Z^2$ , such that  $\alpha \approx \beta - \pi/2$ . To  $\mathcal{O}(\epsilon_{1,2i})$ , the eigenvalues are unchanged from the CP-conserving case. Note that  $m_A$  is now the mass of the “mostly-pseudoscalar” eigenstate, not the mass of  $A_0$ . To avoid this confusion, we will express physical quantities in terms of the charged Higgs boson mass, using the relation

$$m_{H\pm}^2 = m_A^2 + m_W^2 + 2\epsilon_{2r} v^2. \quad (15)$$

The Higgs phase  $\theta$ , determined by the minimization condition  $\partial V_0 / \partial \theta = 0$ , is given by

$$\tan \theta = \frac{2v^2 (\epsilon_{2i} s_{2\beta} - 2\epsilon_{1i})}{s_{2\beta} (m_{H\pm}^2 - m_W^2) + 2v^2 (\epsilon_{2r} s_{2\beta} - 2\epsilon_{1r})}. \quad (16)$$

In the small  $\tan \beta$  regime (such that  $\cot \beta \gg |\epsilon_1| v^2 / m_A^2$ ), one can treat  $\theta$  perturbatively since it is  $\mathcal{O}(\epsilon_{1,2})$ . However, in the large  $\tan \beta$  regime (such that  $\cot \beta \lesssim |\epsilon_1| v^2 / m_A^2$ ), one can have  $\theta = \mathcal{O}(1)$ . In this regime, the Higgs potential can develop more than one minimum in the  $\theta$  direction; we discuss this possibility in Appendix A. In practice, constraints on  $b \rightarrow s \gamma$  [28] imply that the mass of the charged Higgs cannot be too light ( $m_{H\pm} \gtrsim 300 \text{ GeV}$ ) unless the charged Higgs contribution to  $b \rightarrow s \gamma$  interferes destructively with some other process<sup>3</sup>. Restricting ourselves to  $m_{H\pm} > 200 \text{ GeV}$  and  $\tan \beta < 10$  is sufficient to avoid additional phase minima.

---

<sup>3</sup> Some amount of interference is in fact expected, considering the light stops and charginos of our baryogenesis scenario, weakening the bound on  $m_{H\pm}$ .

CP violation from the complex BMSSM parameters  $\epsilon_{1,2}$  also enters the SUSY mass matrices, potentially impacting both baryogenesis and EDMs. For example, the top squark mass matrix, in the  $(\tilde{t}_L^*, \tilde{t}_R^*)$  basis, is

$$\mathbf{m}_{\tilde{t}}^2 = \begin{pmatrix} m_{Q_3}^2 + y_t^2 s_\beta^2 v^2 + \Delta_{\tilde{u}_L} & y_t(A_t^* v_u^* - \mu v_d + 2\epsilon_1 v_u v_d^2 / \mu^*) \\ y_t(A_t v_u - \mu^* v_d^* + 2\epsilon_1^* v_u^* v_d^{*2} / \mu) & m_{\tilde{u}_3}^2 + y_t^2 s_\beta^2 v^2 + \Delta_{\tilde{u}_R} \end{pmatrix} \quad (17)$$

with D-term contributions  $\Delta_\phi = (T_{3\phi} - Q_\phi \sin^2 \theta_W) c_{2\beta} m_Z^2$ . We define the stop mixing parameter  $X_t = |[\mathbf{m}_{\tilde{t}}^2]_{12}|$  as the magnitude of the off-diagonal entry in Eq. (17). The chargino mass matrix, in the  $(\tilde{W}^+, \tilde{H}_u^+, \tilde{W}^-, \tilde{H}_d^-)$  basis, is

$$\mathbf{M}_{\tilde{C}} = \begin{pmatrix} 0 & \mathbf{X}^T \\ \mathbf{X} & 0 \end{pmatrix}, \quad \mathbf{X} = \begin{pmatrix} M_2 & g v_u^* \\ g v_d^* & \mu - 2\epsilon_1 v_d v_u / \mu^* \end{pmatrix}. \quad (18)$$

The neutralino mass matrix, in the  $(\tilde{B}, \tilde{W}^0, \tilde{H}_d^0, \tilde{H}_u^0)$  basis, is

$$\mathbf{M}_{\tilde{N}} = \begin{pmatrix} M_1 & 0 & -g' v_d^* / \sqrt{2} & g' v_u^* / \sqrt{2} \\ 0 & M_2 & g v_d^* / \sqrt{2} & -g v_u^* / \sqrt{2} \\ -g' v_d^* / \sqrt{2} & g v_d^* / \sqrt{2} & 2\epsilon_1 v_u^2 / \mu^* & -\mu + 4\epsilon_1 v_u v_d / \mu^* \\ g' v_u^* / \sqrt{2} & -g v_u^* / \sqrt{2} & -\mu + 4\epsilon_1 v_u v_d / \mu^* & 2\epsilon_1 v_d^2 / \mu^* \end{pmatrix}. \quad (19)$$

In each of these mass matrices, the BMSSM parameters lead to new sources of CP violation through both the explicit factors of  $\epsilon_1$  and the complex phase of the Higgs vevs, depending on  $\epsilon_1$  and  $\epsilon_2$ . Physical CP violation observables depend on these phases only through the invariant combinations listed in Table I.

To summarize, CP violation from the BMSSM manifests in the following ways:

- Mixing arises between CP-even and CP-odd neutral Higgs eigenstates, proportional to  $m_{hA}^2$  and  $m_{HA}^2$ .
- The Higgs phase  $\theta$  enters through the Higgs vevs in the SUSY mass matrices.
- The parameter  $\epsilon_1$  appears explicitly in the SUSY mass matrices.

In Sec. III, we show that the BAU induced through BMSSM phases is approximately proportional to  $\theta$ . In Sec. IV, we find that the dominant contributions to EDMs arise through either  $\theta$  or  $h_0$ - $A_0$  mixing. Since  $\theta$  and  $m_{hA}^2$  are proportional to the same linear combination of  $\epsilon_{1,2i}$ , EDM constraints will provide direct bounds on the EWBG mechanism in the BMSSM.



### III. ELECTROWEAK BARYOGENESIS

In this section, we describe how electroweak baryogenesis is realized in the BMSSM. First, we study the nature of the phase transition and the properties of the expanding bubbles relevant for the BAU computation. Second, we identify novel sources of CP violation in the BMSSM and compute the resulting BAU. The new sources are induced by a variation of the Higgs phase  $\theta$  across the bubble wall. Therefore, we devote special attention to the computation of the temperature and space-time dependence of  $\theta$ . Similar effects arise also in the MSSM at the quantum level [29, 30]. In the BMSSM they arise classically [15], and can be quantitatively much more significant.

#### A. Phase Transition and Bubble Properties

##### 1. The critical vev and temperature

The EWBG mechanism requires a “strong” first-order phase transition to avoid sphaleron erasure of the BAU within the broken phase. This condition is satisfied if [31]

$$\frac{\sqrt{2}v_c}{T_c} > 1, \quad (20)$$

where  $T_c$  is the critical temperature (defined here as the temperature of free-energy degeneracy between the broken and symmetric phases) and  $v_c \equiv v(T_c)$  is the Higgs vev in the broken phase at  $T_c$ , in the normalization of Eq. (8). Since a first-order phase transition in the BMSSM arises through radiative corrections involving stops (as in the MSSM [5, 32]), Eq. (20) provides important constraints on the parameters of the stop sector. In addition, the size of  $v_c$  itself is important for the BAU computation; as we show below, the BAU scales as  $v_c^4$ .

We compute  $v_c$  and  $T_c$  using the two-loop finite-temperature effective potential of Ref. [17], provisionally neglecting the effect of CP violation. In Fig. 1 (left panel), we show how  $T_c$  and  $v_c$  depend on the stop parameters [*c.f.* Eq. (17)]. We consider two cases: mixing ( $X_t = (150 \text{ GeV})^2$ ) and no mixing ( $X_t = 0$ ), while varying  $m_{U_3}^2$  (assuming  $m_{U_3}^2 < 0$ ) and fixing  $m_A = 250 \text{ GeV}$ ,  $\tan \beta = 5$ ,  $m_h = 114 \text{ GeV}$ , and  $m_{Q_3} = 200 \text{ GeV}$ . At a given value of  $m_{U_3}^2$ , stop mixing suppresses  $v_c/T_c$ , thereby weakening the phase transition. The filled circle at the lower edge of the  $X_t > 0$  line (gray) corresponds to the maximal value of  $m_{U_3}^2$  where

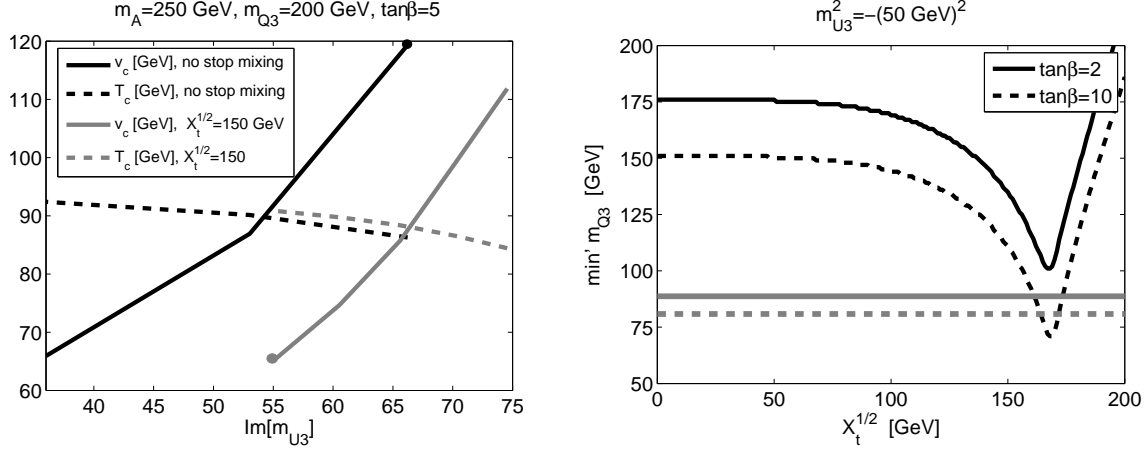


FIG. 1: *Left: The critical vev  $v_c$  (solid curve) and temperature  $T_c$  (dashed) vs. the right-handed stop soft mass  $m_{U_3}$  (imaginary, since  $m_{U_3}^2 < 0$ ), for two values of the mixing parameter  $X_t$ . Right, black: The minimum value of  $m_{Q_3}$ , consistent with the electroweak oblique parameter  $T < 0.2$ , as a function of the stop mixing  $\sqrt{X_t}$ , for two values of  $\tan\beta$ . Gray: Model independent, direct limit from sbottom search.*

Eq. (20) is fulfilled. On the other hand, decreasing  $m_{U_3}^2$  increases  $v_c/T_c$ , strengthening the phase transition; eventually, however, this leads to an undesirable tachyonic stop, denoted by the filled circle at the upper edge of the  $X_t = 0$  line (black). These effects are well known in the MSSM: stop mixing effectively screens the one-loop cubic correction to the effective potential and increases the value of the Higgs mass, while such screening can be compensated by a sufficiently negative  $m_{U_3}^2$ .

Next, we consider how the strength of the phase transition depends on  $m_{Q_3}$ . We vary  $m_{Q_3}$  while keeping the neutral Higgs mass fixed by simultaneously adjusting  $\epsilon_{1,2r}$ . For  $m_{Q_3} > 200$  GeV,  $v_c$  and  $T_c$  are only weakly dependent on  $m_{Q_3}$ . For  $m_{Q_3} < 200$  GeV, the phase transition is strengthened as one decreases  $m_{Q_3}$ , allowing for Eq. (20) to be consistent with greater values of  $m_{U_3}^2$  [15, 17]. However, experimental constraints provide a lower bound on  $m_{Q_3}$ , shown in Fig. 1 (right panel). The collider search bound on bottom squarks ( $m_{\tilde{b}} > 89$  GeV [4]) implies that  $m_{Q_3} \gtrsim 80$  GeV [17], shown in gray <sup>4</sup>. The precision constraint on the  $\rho$  parameter, which is sensitive to the  $\mathcal{O}(m_t^2/m_{Q_3}^2)$  relative mass splitting in the doublet

<sup>4</sup> For a neutralino LSP with mass  $m_{\chi_1^0} \lesssim 90$  GeV, the bound is significantly stronger:  $m_{\tilde{b}} \gtrsim 250$  GeV [33].

$(\tilde{t}_L, \tilde{b}_L)$ , provides a stronger bound [3, 4]. We find that  $m_{Q_3} \gtrsim 160$  GeV is required at the 95% CL, unless the stops are substantially mixed; at the 90% CL one must keep  $m_{Q_3} \gtrsim 200$  GeV.

## 2. The bubble profiles

We now turn to the properties of the bubbles that nucleate and expand during the phase transition [34, 35]. These bubbles are characterized by spacetime-dependent background Higgs fields, described by  $(v, \beta, \theta)$ . In the MSSM, the dominant sources driving EWBG are proportional to the small parameter  $\Delta\beta \lesssim 10^{-2}$  associated with the spacetime variation of  $\beta$  [34]. Here, we neglect variation in  $\beta$  ( $\Delta\beta = 0$ ) in order to focus on the leading BMSSM effects proportional to the analogous parameter  $\Delta\theta$  associated with variation of  $\theta$  across the bubble wall.

The bubble profiles for  $v$  and  $\theta$  are determined by equations of motion

$$\frac{\partial V_T}{\partial v} = 2 \frac{\partial^2 v(z)}{\partial z^2} \quad (21a)$$

$$\frac{\partial V_T}{\partial \theta} = \frac{s_{2\beta}^2}{2} \partial_z (v^2(z) \partial_z \theta(z)) \quad , \quad (21b)$$

assuming a vanishing  $Z$  background [30, 36]. Here,  $V_T$  is the finite temperature effective potential and the coordinate  $z$  is the distance from the wall in its rest frame (we assume a planar bubble). The boundary conditions are such that  $z = +\infty (-\infty)$  corresponds to the broken (unbroken) minimum of the potential.

Rather than solving Eq. (21a), we assume a kink ansatz for the Higgs vev:

$$v(z) = \frac{v(T)}{2} \left[ 1 + \tanh \left( \frac{2z}{L_w} \right) \right] \quad (22)$$

To avoid complication, we set  $v(T) = v_c$ . This potentially underestimates the BAU: since the time of bubble growth necessarily corresponds to  $T < T_c$ , one in general expects  $v(T) > v_c$ , resulting with more effective sources. The approximation is justified if, following the onset of the phase transition, the universe is reheated back near the critical temperature [37, 38].

The wall width  $L_w$  is defined to match the kink ansatz of Eq. (22) onto the bubble profile,

$$L_w = \int_{v_{\min}}^{v_{\max}} \frac{d\phi}{\sqrt{V_T(\phi)}} \quad , \quad (23)$$

where  $v_{\min} = 0.1 v_c$  and  $v_{\max} = 0.9 v_c$  designate the field on either side of the wall. Neglecting CP violation in Eq. (23), we find values in the range  $L_w = (15 - 40)/T_c$ .

Next, we obtain the profile of the vev phase  $\theta(z)$ . In order to clearly illustrate the essential dynamics, we make two simplifications: (i) we consider the  $\theta \ll 1$  regime, satisfied when  $\cot \beta \gg |\epsilon_1|v^2/m_A^2$ , and (ii) we neglect all radiative corrections to the phase-dependent part of  $V_T$ . Under these assumptions, Eq. (21b) becomes

$$\partial_z \left( v^2(z) \partial_z \theta(z) \right) \approx v^2(z) (m_{H^\pm}^2 - m_W^2) \left[ \theta(z) - \frac{v^2(z)}{v_0^2} \theta_0 \right]. \quad (24)$$

In the present section, the zero temperature Higgs phase and vev are denoted  $\theta_0$  and  $v_0$  for clarity. Eq. (24) can be cast in the dimensionless form

$$\partial_r (g \partial_r f) = \tau g (f - g), \quad (25)$$

where

$$f(z) \equiv \frac{v_c^2 \theta(z)}{v_0^2 \theta_0}, \quad r \equiv \frac{2z}{L_w}, \quad \tau \equiv \frac{L_w^2 (m_{H^\pm}^2 - m_W^2)}{4}, \quad g(r) \equiv \left( \frac{1 + \tanh r}{2} \right)^2. \quad (26)$$

For  $m_{H^\pm} > 200$  GeV, we have  $\tau > 100$ . Thus, the solution to Eq. (25) is governed by the potential energy term on the RH side, such that  $f(r) \approx g(r) + \mathcal{O}(\tau^{-1})$ . This conclusion is borne out by numerical evaluations for  $\tau > 30$ , which we perform using the method of Ref. [39].

In summary, the Higgs phase profile is given by

$$\theta(z) \approx \frac{\Delta\theta}{4} \left[ 1 + \tanh \left( \frac{2z}{L_w} \right) \right]^2 \quad (27)$$

where  $\Delta\theta \approx \theta_0 v_c^2 / v_0^2$ . We note that  $\theta(z)$  is proportional to the square of the kink in Eq. (22), not linear. Furthermore, since EDMs are directly sensitive to the value of  $\theta_0$ , this sensitivity translates into a direct constraint on the phase variation across the bubble wall, and hence on baryogenesis.

The preceding analysis can be generalized away from the  $\theta \ll 1$  regime, necessary when  $\tan \beta \gtrsim 10$ . Assuming that the profile of  $\theta$  is again dominated by potential energy (such that  $\partial V_T / \partial \theta \approx 0$ ), we find the following approximate solution for  $\theta(z)$ :

$$\tan(\theta(z) - \theta_0) \approx \frac{2(s_{2\beta} \epsilon_{2i} - 2\epsilon_{1i})(v(z)^2 - v_0^2)}{s_{2\beta}(m_{H^\pm}^2 - m_W^2) + 4\epsilon_{1r}(v(z)^2 - v_0^2)}. \quad (28)$$

This solution gives the leading behavior of  $\theta(z)$  in all  $\tan \beta$  regimes: (i) it reduces to Eq. (27) when  $\cot \beta \gg |\epsilon_1|v^2/m_A^2$  limit, and (ii) it is valid to leading order in  $\cot \beta$  when  $\cot \beta \lesssim |\epsilon_1|v^2/m_A^2$ .

In Appendix B, we study the impact of radiative corrections on the Higgs phase at zero and finite temperature. In particular, we find that  $\theta(z)$  is shifted by an overall constant, while  $\Delta\theta$  remains approximately unchanged.

### 3. Wall velocity

The bubble wall velocity is an important parameter in the EWBG computation. A recent study found that  $v_w \sim 0.4$  in the MSSM [40], significantly larger than previous estimates of  $v_w \sim 0.01-0.1$  [41]. Therefore it is worthwhile examining how the BAU depends on  $v_w$ .

The optimal wall velocity for EWBG arises as a competition between two Sakharov conditions. The generation of baryon number ( $n_B$ ) is fueled by chiral charge diffusing ahead of the advancing bubble wall, characterized by an effective diffusion constant  $\bar{D}$  and a diffusion time  $\tau_{\text{diff}} = \bar{D}/v_w^2$  [42]. If electroweak sphalerons are in equilibrium, with rate  $\Gamma_{\text{ws}} \gg \tau_{\text{diff}}^{-1}$ ,  $n_B$  is suppressed, as per the third Sakharov condition. On the other hand, if  $\Gamma_{\text{ws}} \ll \tau_{\text{diff}}^{-1}$ , then  $n_B$  is also suppressed, since few baryon number violating processes occur. Therefore, the maximum baryon number production occurs when  $\Gamma_{\text{ws}} \sim \tau_{\text{diff}}^{-1}$ , corresponding to a velocity  $v_w \sim \sqrt{\bar{D}\Gamma_{\text{ws}}} \sim (\text{few}) \times 10^{-2}$  [38]. In our numerical computation, described below, we indeed find that  $n_B$  is maximized for  $v_w = 0.03$ .

If we consider the range  $0.01 < v_w < 0.4$ , we find  $n_B$  varies by a factor of 4–5, with the minimum  $n_B$  for  $v_w = 0.4$ . For the sake of definiteness, we fix  $v_w = 0.1$ , which is approximately the central value for  $n_B$ . We expect that  $v_w$  in the BMSSM can be approximated by the MSSM case. Potentially, the presence of the light LH stop leads to an additional contribution to the frictional force determining  $v_w$ . However, we expect this to be a minor effect since  $\tilde{t}_L$ , which cannot be too light, is somewhat Boltzmann suppressed and acquires only a fraction of its mass via the Higgs mechanism.

## B. Baryon Asymmetry Computation

The computation of the BAU involves a system of coupled Boltzmann equations of the form

$$\partial_t n_a - D_a \nabla^2 n_a = \sum_b \Gamma_{ab} n_b + S_a^{\text{CP}}. \quad (29)$$

Here  $n_a$  is the charge density for species  $a$ . The CP-violating source  $S_a^{\varphi\mathbb{P}}$ , non-zero only within the moving bubble wall, leads to the generation of non-zero  $n_a$ . The diffusion constant  $D_a$  describes how efficiently  $n_a$  is transported ahead of the wall into the unbroken phase where sphalerons are active. The interaction coefficients  $\Gamma_{ab}$  correspond to (i) inelastic processes that convert charge from one species to another, and (ii) relaxation processes that wash out charge within the broken phase. Although BMSSM contributions modify  $\Gamma_{ab}$  at  $\mathcal{O}(\epsilon_{1,2})$ , it is safe to neglect these corrections. Previous studies have shown that the solutions to the Boltzmann equations are insensitive to sub- $\mathcal{O}(1)$  variations in the interaction coefficients [42–44]. We refer the reader to Ref. [43, 44], which we follow here, for details concerning the setup and derivation of the Boltzmann equations in the MSSM.

### 1. CP-violating sources

The novelty of BMSSM baryogenesis appears in the CP-violating sources. We compute these sources following the “vev-insertion” approach of Refs. [45, 46]. More sophisticated treatments, going beyond the vev-insertion approximation, exist in the literature [47, 48]. However, there remains some controversy, and this is an area of active investigation [49]. Therefore, we opt for the simplest framework (vev-insertion) by which we may present our new BMSSM sources.

The higgsino CP-violating source, which drives EWBG in the MSSM, receives important BMSSM contributions. We have

$$S_{\tilde{H}}^{\varphi\mathbb{P}}(z) = \frac{3g^2 K_2(z)}{2\pi^2} \int_0^\infty \frac{k^2 dk}{\omega_{\tilde{W}} \omega_{\tilde{H}}} \text{Im} \left[ \frac{n_F(\mathcal{E}_{\tilde{W}}) - n_F(\mathcal{E}_{\tilde{H}}^*)}{(\mathcal{E}_{\tilde{W}} - \mathcal{E}_{\tilde{H}}^*)^2} + \frac{1 - n_F(\mathcal{E}_{\tilde{W}}) - n_F(\mathcal{E}_{\tilde{H}}^*)}{(\mathcal{E}_{\tilde{W}} + \mathcal{E}_{\tilde{H}}^*)^2} \right] \\ + \frac{g'^2 K_1(z)}{2\pi^2} \int_0^\infty \frac{k^2 dk}{\omega_{\tilde{B}} \omega_{\tilde{H}}} \text{Im} \left[ \frac{n_F(\mathcal{E}_{\tilde{B}}) - n_F(\mathcal{E}_{\tilde{H}}^*)}{(\mathcal{E}_{\tilde{B}} - \mathcal{E}_{\tilde{H}}^*)^2} + \frac{1 - n_F(\mathcal{E}_{\tilde{B}}) - n_F(\mathcal{E}_{\tilde{H}}^*)}{(\mathcal{E}_{\tilde{B}} + \mathcal{E}_{\tilde{H}}^*)^2} \right]. \quad (30)$$

The first and second terms correspond to the sources induced through higgsino-wino and higgsino-bino mixing, respectively. The important BMSSM effects enter into the prefactors

$$K_i(z) = |M_i \mu| v^2(z) \left[ \sin(\phi_i + \theta(z)) \dot{\beta}(z) + \frac{s_{4\beta}}{4} \cos(\phi_i + \theta(z)) \dot{\theta}(z) \right], \quad (31)$$

where  $M_{1,2}$  are the gaugino mass parameters. In the MSSM we have  $\theta = \dot{\theta} = 0$ , so that the sources are driven by the gaugino phases  $\phi_i$  defined in Table I. However, in the BMSSM,

contributions arise from  $\epsilon_{1,2i}$ , entering through  $\theta$ . Furthermore, the second term in Eq. (31), which is unique to the BMSSM, is not suppressed by  $\Delta\beta \lesssim 10^{-2}$ . The momentum integrals in Eq. (30) are identical to the MSSM case, discussed in Ref. [46]; roughly speaking, they are maximized “on-resonance” (when  $|M_i| \sim |\mu|$ ) and are highly suppressed far off-resonance.

In the MSSM, the CP-violating sources for third generation squarks cannot drive EWBG. The Higgs mass bound requires that  $\tilde{t}_L$  and  $\tilde{b}_L$  are heavy, and thereby Boltzmann suppressed in the electroweak plasma. The BMSSM opens the door for squark-driven baryogenesis, since the stops and sbottoms can be relatively light. The CP-violating sources for stops ( $\tilde{q} = \tilde{t}$ ) and sbottoms ( $\tilde{q} = \tilde{b}$ ) are

$$\begin{aligned} S_{\tilde{q}R}^{\mathcal{CP}} &= - S_{\tilde{q}L}^{\mathcal{CP}} \\ &= \frac{3y_q^2 K_{\tilde{q}}(z)}{2\pi^2} \int_0^\infty \frac{k^2 dk}{\omega_{\tilde{q}L} \omega_{\tilde{q}R}} \text{Im} \left[ \frac{n_B(\mathcal{E}_{\tilde{q}R}^*) - n_B(\mathcal{E}_{\tilde{q}L})}{(\mathcal{E}_{\tilde{q}L} - \mathcal{E}_{\tilde{q}R}^*)^2} + \frac{1 + n_B(\mathcal{E}_{\tilde{q}R}) + n_B(\mathcal{E}_{\tilde{q}L})}{(\mathcal{E}_{\tilde{q}L} + \mathcal{E}_{\tilde{q}R})^2} \right], \end{aligned} \quad (32)$$

with prefactor

$$\begin{aligned} K_{\tilde{q}}(z) &= |A_q \mu| v^2(z) \dot{\beta}(z) \sin(\phi_q + \theta(z)) \\ &\quad + \frac{v^2(z)}{4} (s_{4\beta} |A_q \mu| \cos(\phi_q + \theta(z)) + s_{2\beta}^2 (|\mu|^2 - |A_t|^2)) \dot{\theta}(z). \end{aligned} \quad (33)$$

In addition to the squark phases  $\phi_q$  appearing in Table I, the CP-violating sources include contributions from  $\epsilon_{1,2i}$  that enter through  $\theta$ .

In the BMSSM, there are CP-violating sources for the third generation quarks, top ( $q = t$ ) and bottom ( $q = b$ ), due to the Higgs phase  $\theta(z)$ , that does not arise in the MSSM:

$$\begin{aligned} S_{qR}^{\mathcal{CP}} &= - S_{qL}^{\mathcal{CP}} = \frac{3y_q^2 K_q(z)}{2\pi^2} \int_0^\infty dk k^2 \\ &\quad \times \text{Im} \left[ Z_{qL}^p Z_{qR}^h \frac{n_F(\mathcal{E}_{qR}^{h*}) - n_B(\mathcal{E}_{qL}^p)}{(\mathcal{E}_{qL}^p - \mathcal{E}_{qR}^{h*})^2} + Z_{qL}^p Z_{qR}^p \frac{1 + n_B(\mathcal{E}_{qR}^p) + n_B(\mathcal{E}_{qL}^p)}{(\mathcal{E}_{qL}^p + \mathcal{E}_{qR}^p)^2} + (p \leftrightarrow h) \right]. \end{aligned}$$

where

$$K_q(z) = -v^2(z) s_{2\beta}^2 \dot{\theta}(z). \quad (34)$$

Again, we refer to Ref. [46] for the notation of quantities within the momentum integral. We note that because the quark thermal masses and widths are approximately equal for  $q_L$  and  $q_R$  (dominated by common QCD effects), the momentum integral is suppressed. This situation may be an artifact of the vev-insertion approach. Similar quark CP-violating sources, computed within the WKB approximation, have been studied within the contexts of Two Higgs Doublet models [50] and the SM with higher dimensional operators [51].

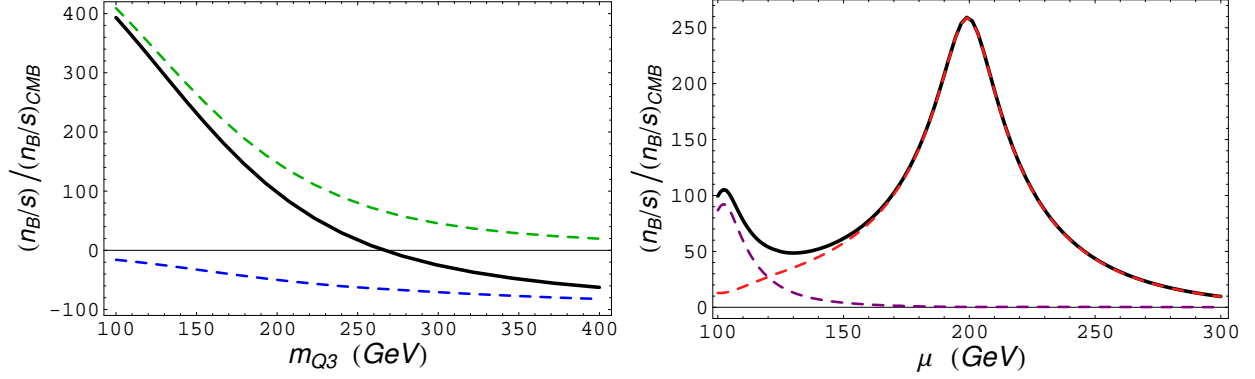


FIG. 2: The baryon asymmetry generated by  $\dot{\theta}$ -terms in CP-violating sources in units of the observed BAU. Left panel: top source (blue, dashed), stop source (green, dashed), and their sum (black, solid) as a function of the soft LH stop mass parameter. Right panel: higgsino-bino source (purple, dashed), higgsino-wino source (red, dashed), and their sum (black, solid) as a function of  $\mu$ . Other relevant parameters are specified in Table II.

## 2. The baryon asymmetry

Here, we compute the baryon asymmetry. As argued above, we expect that the leading BMSSM effects will enter through the CP-violating sources. We neglect BMSSM effects arising in the various transport coefficients and diffusion constants that enter the Boltzmann equations, following the general MSSM setup described in Ref. [44]. In addition, we make the further assumption of chemical equilibrium between particles and their superpartners, valid when gauginos have masses  $M_i \lesssim 1$  TeV. We include transport coefficients for bottom and tau Yukawa interactions, recently shown to play an important role in MSSM baryogenesis [42].

The BMSSM CP-violating sources can have a large impact on baryon number generation, illustrated in Fig. 2. Here, we plot  $n_B/s$  (the baryon-to-entropy-density ratio), normalized to the observed value  $n_B/s \simeq 9 \times 10^{-11}$  [52], for maximal  $\Delta\theta$ ; *i.e.*, the vertical axis approximately shows  $1/\Delta\theta$  needed to give the observed BAU. In order to highlight the novel effects of the BMSSM, we take  $\Delta\beta = 0$  and neglect all MSSM phases ( $\phi_i = \phi_q = 0$ ). The  $\dot{\theta}$  contributions are suppressed in the large  $\tan\beta$ -limit; we take  $\tan\beta = 3$ . Other parameters are specified in Table II.

In the left panel of Fig. 2, we show the BAU induced via  $\dot{\theta}$  contributions to the top (blue



dashed) and stop (green dashed) CP-violating sources, as a function the left-handed stop mass parameter  $m_{Q_3}$ . Since the right-handed stop is light, the stop source is enhanced for smaller values of  $m_{Q_3}$  due to the resonance of the CP-violating source. The stop source becomes suppressed off-resonance, for large  $m_{Q_3}$ . The top CP-violating source does not depend on  $m_{Q_3}$ . However, the top-driven contribution to  $n_B/s$  is suppressed at small values of  $m_{Q_3}$  due to (i) an enhanced stop contribution to the relaxation rate [46], and (ii) more charge equilibrating into left-handed stops, rather than tops, reducing the fermionic charge available for sphaleron conversion.

In the right panel of Fig. 2, we show the BAU induced via  $\dot{\theta}$  contributions to the higgsino-wino (red dashed) and higgsino-bino (purple dashed) CP-violating sources. Both sources are enhanced on-resonance when  $\mu \approx M_{1,2}$ . In addition, we have studied the bottom and sbottom CP-violating sources (not shown); though similar to the top/stop contributions, they are suppressed by  $(m_b/m_t)^2$  and would be viable only for  $\Delta\theta = \mathcal{O}(1)$ .

The total baryon asymmetry in the BMSSM is a combination of (i) contributions shown in Fig. 2, and (ii) standard MSSM contributions induced through  $\Delta\beta$  and the MSSM phases. Our key point is that the BMSSM contributions can be large, thereby extending the window in parameter space that can provide successful EWBG. In the next section, we investigate the EDM constraints on this scenario.

## IV. ELECTRIC DIPOLE MOMENTS

### A. EDMs from BMSSM Phases

EDM searches are sensitive to the same CP-violating phases that generate the BAU, and consequently provide powerful constraints on the EWBG mechanism. Currently, the most significant EDM bounds are for the neutron and the thallium and mercury atoms [53–55],

$\mu$	$M_1$	$M_2$	$M_3$	$m_{Q_3}$	$m_{\bar{u}_3}$	$m_{\bar{d}_3}$	$m_{H_{\pm}}$	$v_c$	$T_c$	$L_w^{-1}$
400	100	200	500	300	$\sqrt{-60^2}$	500	350	70	90	3

TABLE II: *The parameters used for Fig. 2, in units of GeV. In addition, we take  $A_t = A_b = 0$ ,  $\tan\beta = 3$ , and all other soft SUSY-breaking masses to be heavier than 1 TeV.*

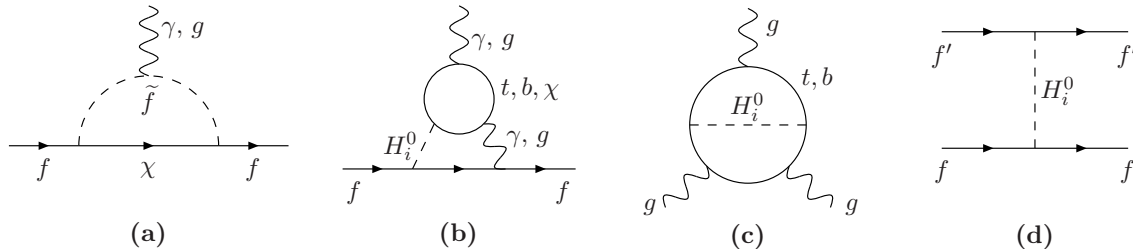


FIG. 3: *Examples of BMSSM contributions to CP-violating operators: (a) one-loop and (b) two-loop EDM and chromo-EDM, (c) Weinberg operator, and (d) four-fermion operator.*

given at 95% C.L.:

$$|d_n| < 3.5 \times 10^{-26} \text{ e cm} , \quad (35a)$$

$$|d_{\text{Tl}}| < 1.1 \times 10^{-24} \text{ e cm} , \quad (35b)$$

$$|d_{\text{Hg}}| < 2.9 \times 10^{-29} \text{ e cm} . \quad (35c)$$

In many scenarios, including in our present work, the electron EDM  $d_e$  provides the dominant contribution to  $d_{\text{Tl}}$ , given by  $d_{\text{Tl}} \simeq -585 d_e$ . Under this assumption, the corresponding bound is  $|d_e| < 1.9 \times 10^{-27} \text{ e cm}$  [95% C.L.].

CP violation in the BMSSM generates, below the weak scale, several classes of CP-violating, non-renormalizable operators, which in turn give rise to the above EDMs [56]. In Fig. 3, we show examples of BMSSM contributions to these operators. At dimension five, there are EDM and chromo-EDM operators, arising at one-loop order (Fig. 3a). Two-loop contributions (Fig. 3b) become dominant when first and second generation sfermions are heavy ( $m_{\tilde{f}} \gtrsim 1 \text{ TeV}$ )<sup>5</sup>. At dimension six, there are the Weinberg operator (Fig. 3c) [57] and four-fermion operators (Fig. 3d). Novel BMSSM contributions to these operators arise from (i) explicit factors of  $\epsilon_{1i}$  in the mass terms for sfermions and higgsinos [Eqs. (17-19)], (ii) tree-level scalar-pseudoscalar neutral Higgs mixing [Eq. (12)], and (iii) the complex Higgs vev, also arising at tree-level [Eq. (16)]. These contributions give rise to irreducible EDMs that cannot be universally suppressed without also destroying the viability of EWBG (barring fine-tuned cancellations).

<sup>5</sup> In the BMSSM, one must not push the first and second generation sfermion masses above the scale  $M$ , where the BMSSM ceases to be valid. In principle, one could consider a modified version of the BMSSM in which these sfermions are integrated out along with the physics responsible for the BMSSM operators.

We evaluate these EDMs following Ref. [58]. This treatment, utilized for the MSSM with a loop-induced CP-violating Higgs sector, includes all four classes of contributions shown in Fig. 3 and allows for the inclusion of the BMSSM effects described above. However, our EDM results are subject to two main theoretical uncertainties. First, the two-loop EDM and chromo-EDM contributions are incomplete; the remaining known MSSM contributions [59–61] have not been generalized to include scalar-pseudoscalar Higgs mixing and cannot be easily adapted to the BMSSM. Second, there exist  $\mathcal{O}(1)$  uncertainties in the hadronic inputs needed for the evaluation of  $d_{\text{Hg}}$  and  $d_n$ . For the neutron, in particular, there exist three different methods for computing  $d_n$ , each sensitive to a different linear combination of CP-violating operators. Below, we show only neutron EDM bounds computed using the more recent “QCD Sum Rules” method, which is sensitive to first generation EDM, chromo-EDM, and Weinberg operators [62].

As we show below, the mercury EDM provides the strongest bound on EWBG in the BMSSM. (In contrast, EWBG in the MSSM is constrained by  $d_e$  and  $d_n$  and is largely insensitive to  $d_{\text{Hg}}$ .) This scenario will be decisively probed by the combination of future EDM searches, which are expected to reach sensitivities of  $10^{-28} e \text{ cm}$  for  $d_n$ ,  $10^{-29} e \text{ cm}$  for  $d_e$ , and  $10^{-29} e \text{ cm}$  for the EDMs of the deuteron ( $d_D$ ) and proton [63].

## B. Constraints on BMSSM Baryogenesis

In this section, we show how limits on EDMs constrain BMSSM baryogenesis. Although both MSSM and BMSSM phases, listed in Table I, can impact both EWBG and EDMs, we choose to highlight the BMSSM by setting all MSSM phases to zero. In this case, CP violation is governed by the parameters  $\epsilon_{1i}$  and  $\epsilon_{2i}$ .

BMSSM baryogenesis can be driven by squark, quark, or higgsino CP-violating sources, discussed in Sec. III. In Figs. 4 and 5, we illustrate how current EDM constraints impact each of these EWBG scenarios, with parameters given in Table III. In each panel, the gray bands show the region of the  $\epsilon_{1i}$ - $\epsilon_{2i}$  parameter space consistent with generating the observed baryon asymmetry. BMSSM baryogenesis is inconsistent with  $\epsilon_{1i} = \epsilon_{2i} = 0$  (shown by the cross), since clearly CP violation is required to generate the BAU. The width of this region corresponds to the following range for the wall velocity  $v_w$  and Higgs vev at the critical

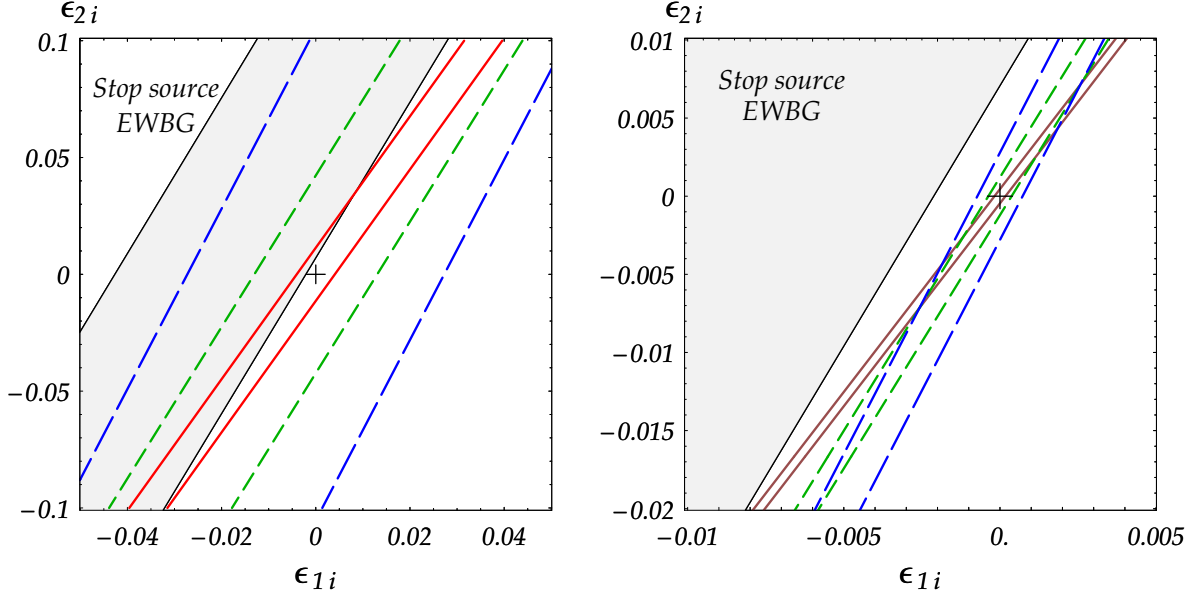


FIG. 4: The viable region for stop-driven EWBG in the  $\epsilon_{1i}$ - $\epsilon_{2i}$  parameter space (in gray), and EDM constraints from  $d_{Hg}$  (red solid),  $d_n$  (green short-dash),  $d_e$  (blue long-dash), and  $d_D$  (brown solid). Left panel: current EDM constraints; Right panel: future EDM constraints:  $|d_n| < 10^{-27} e$  cm,  $|d_e| < 5 \times 10^{-29} e$  cm,  $|d_D| < 10^{-28} e$  cm. (Note: zoomed-in scale on right.) Other relevant parameters are specified in Table III.

temperature  $v_c$  (c.f. Sec. III):

$$0.01 < v_w < 0.4, \quad 70 \text{ GeV} < v_c < 110 \text{ GeV}. \quad (36)$$

The edge of the EWBG region closest to the origin corresponds to the minimum value of  $(\epsilon_{1i} - \sin 2\beta \epsilon_{1i})$  consistent with the BAU, achieved when EWPT parameters fortuitously maximize the CP-violating sources ( $v_w \sim 0.03$  and  $m_{U_3}^2$  such that the  $v_c$  is largest).

In Fig. 4 we consider the stop-driven EWBG scenario. In the left panel, the regions consistent with current mercury, neutron and electron EDM constraints (95% C.L.) lie between the red (solid), green (short dash) and blue (long dash) curves, respectively. Each EDM is consistent with  $\epsilon_{1i} = \epsilon_{2i} = 0$ . Since the EWBG and EDM bands overlap, this scenario is viable in the BMSSM. (In the MSSM, it is not viable, since  $m_{Q_3} \gg 1$  TeV [6].) In the right panel, we illustrate how future improvements in EDM sensitivities can exclude this scenario, assuming null results. Again, we show the same EWBG band, now zoomed in. The EDM bounds correspond to  $|d_e| < 5 \times 10^{-29} e$  cm (blue long dash),  $|d_n| < 10^{-27} e$  cm (green short

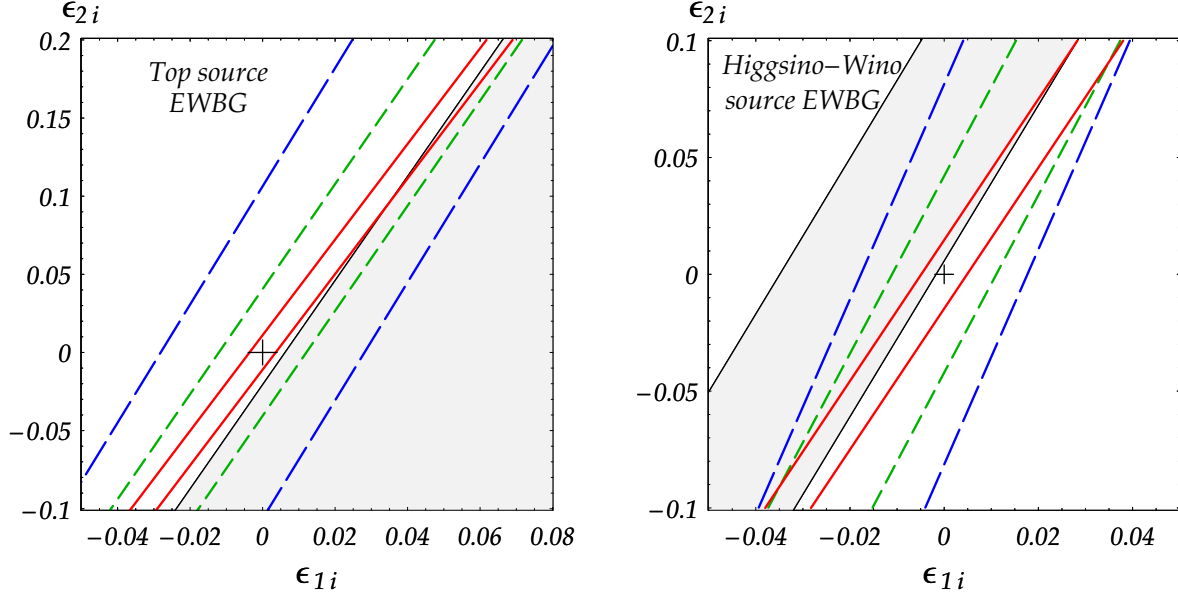


FIG. 5: The viable region for top-driven (left) and higgsino-wino driven (right) EWBG in the  $\epsilon_{1i}$ - $\epsilon_{2i}$  parameter space (in gray), and EDM constraints from  $d_{H_g}$  (red solid),  $d_n$  (green short-dash), and  $d_e$  (blue long-dash). Other relevant parameters are specified in Table III.

dash), and  $|d_D| < 10^{-28} e \text{ cm}$  (brown solid). EWBG is excluded within the intersection of these bounds. Furthermore, these are pessimistic limits compared to actual expected future experimental sensitivities (described above). Of course, the alternative, that EDMs will be discovered, is a much more exciting prospect.

In Fig. 5, we consider EWBG scenarios driven by a top CP-violating source (left) and higgsino-wino source (right). As above, viable EWBG can occur in the gray region, while the current EDM constraints are shown by the colored bands, as in Fig. 5.

Strikingly, the bands for EWBG and EDMs in Figs. 4 and 5 appear to align in the  $\epsilon_{1i}$ - $\epsilon_{2i}$

EWBG scenario	$m_{Q_3}$	$m_{\bar{u}_3}$	$m_{\bar{d}_3}$	$m_{H_{\pm}}$	$\mu$	$M_1$	$M_2$	$M_3$
squark-driven	150	$\sqrt{-60^2}$	500	350	400	100	200	1000
quark-driven	500	$\sqrt{-60^2}$	500	350	400	100	200	1000
wino-driven	400	$\sqrt{-60^2}$	500	350	200	100	200	1000

TABLE III: The parameters used for Figs. 4 and 5 in units of GeV. We take  $\tan \beta = 3$ ,  $\epsilon_{1r} = -0.05$ ,  $\epsilon_{2r} = 0.05$ ,  $A_f = 0$ , and  $m_f^2 = (1 \text{ TeV})^2$  for all other sfermion masses-squared.

plane, signaling that they depend largely on the same linear combination of  $\epsilon_{1,2i}$ . The BAU is proportional to  $\Delta\theta$ , the variation of the Higgs phase across the wall, while the EDMs are dominated by contributions proportional to  $m_{hA}^2$  (the  $h_0$ - $A_0$  mixing parameter) or  $\theta$  (the vacuum Higgs phase). Indeed, all three parameters are approximately proportional to  $(2\epsilon_{1i} - \sin 2\beta \epsilon_{2i})$ .

The mercury EDM limit provides the strongest constraint on EWBG in the BMSSM. Here, the dominant contribution to  $d_{\text{Hg}}$  is the down quark chromo-EDM operator induced at two-loop (Fig. 3b) with a top quark loop and light Higgs exchange, proportional to the  $h_0$ - $A_0$  mixing parameter  $m_{hA}^2$ . The subdominant contribution proportional to  $m_{HA}^2$  is responsible for the slight skew between the  $d_{\text{Hg}}$  and EWBG bands in Fig. 4.

Lastly, we describe how EWBG and EDMs depend on the parameters  $m_A$  and  $\tan\beta$ . The consistency between EDMs and EWBG is generally insensitive to  $m_A$ . Larger values of  $m_A$  suppress  $\Delta\theta$  and the baryon asymmetry as  $\sim 1/m_A^2$ , requiring larger values of  $\epsilon_{1,2i}$ , but the EDMs bounds are correspondingly weakened as well. On the other hand, for larger values of  $\tan\beta$ , the BMSSM CP-violating sources are either constant or suppressed, while EDMs become enhanced — thus leading to stronger constraints on this scenario.

## V. CONCLUSIONS

Adding dimension-five terms to the Higgs potential of the supersymmetric standard model alleviates the fine-tuning problem related to the LEP lower bound on the Higgs mass, and has interesting consequences for the electroweak phase transition and dark matter.

Here, we have investigated the consequences of the new CP-violating phases of these terms for supersymmetric baryogenesis and electric dipole moments. Our main observations and conclusions are the following:

1. The introduction of the  $\epsilon_1$  and  $\epsilon_2$  terms implies two new physical CP-violating phases.
2. Unlike the MSSM, the BMSSM allows for spontaneous baryogenesis, that is baryogenesis that is generated by a complex phase in the Higgs VEVs that is changing across the bubble wall.
3. In addition, several CP-violating sources that are ineffective in the MSSM, can become effective in the BMSSM, namely the stop and top sources.

4. It is possible to have successful baryogenesis with all the MSSM phases put to zero, and with either or both of the two new phases.
5. The EDM constraints can be satisfied if the new phases are of order 0.1 or smaller. Successful baryogenesis requires, however, that they are not much smaller than the EDM upper bound. Thus, barring cancellations, BMSSM baryogenesis predicts that EDMs should be discovered if the experimental sensitivity improves by about an order of magnitude.

## Appendix A: Higgs phase vacua

In this appendix we discuss the vacuum value of the Higgs phase  $\theta$ . At tree level, the part of the Higgs potential which depends on  $\theta$  is

$$\Delta V_0 = -v^2 \sin 2\beta \operatorname{Re} \left[ e^{i\theta} (|b| + 2|\epsilon_1|v^2 e^{i\vartheta_1}) - e^{i(\vartheta_2+2\theta)} \frac{|\epsilon_2|v^2 \sin 2\beta}{2} \right]. \quad (\text{A1})$$

At fixed values of  $v$  and  $\tan \beta$ , the vacuum structure in the  $\theta$  direction is determined by a single complex parameter. To see this, define the following quantities:

$$\begin{aligned} b_{\text{eff}} &= |b| + 2|\epsilon_1|v^2 e^{i\vartheta_1}, \\ \vartheta_{\text{eff}} &= \arg[b_{\text{eff}}], \\ |A| &= |b_{\text{eff}}|v^2 \sin 2\beta, \\ \kappa &= -\left| \frac{\epsilon_2}{b_{\text{eff}}} \right| v^2 \sin 2\beta e^{i(\vartheta_2-2\vartheta_{\text{eff}})}, \\ \tilde{\theta} &= \theta + \vartheta_{\text{eff}}. \end{aligned} \quad (\text{A2})$$

The potential and the minimum equations can be written as

$$\Delta V_0(\tilde{\theta}) = -|A| \operatorname{Re} \left[ e^{i\tilde{\theta}} + \frac{\kappa}{2} e^{2i\tilde{\theta}} \right], \quad (\text{A3a})$$

$$\partial_{\tilde{\theta}} \Delta V_0(\tilde{\theta}) = +|A| \operatorname{Im} \left[ e^{i\tilde{\theta}} + \kappa e^{2i\tilde{\theta}} \right] = 0, \quad (\text{A3b})$$

$$\partial_{\tilde{\theta}}^2 \Delta V_0(\tilde{\theta}) = +|A| \operatorname{Re} \left[ e^{i\tilde{\theta}} + 2\kappa e^{2i\tilde{\theta}} \right] > 0. \quad (\text{A3c})$$

Eq. (A3) admits an analytic solution, depending only on  $\kappa$ . The solution is obtained noting that Eq. (A3b) can be cast as a quartic equation  $\sum_{i=0}^4 a_i \sin^i \tilde{\theta} = 0$ , with coefficients  $a_0 = \operatorname{Im}[\kappa]^2$ ,  $a_1 = 2\operatorname{Im}[\kappa]$ ,  $a_2 = 1 - 4|\kappa|^2$ ,  $a_3 = -4\operatorname{Im}[\kappa]$ ,  $a_4 = 4|\kappa|^2$ . Out of the four roots of the quartic equation, at most two represent a local minimum of the potential.

In order for a double well potential to arise, the  $\epsilon_2$  term must be sizable in comparison with  $b_{\text{eff}}$ . In particular, for  $|\kappa| < 1/2$ , only one minimum exists regardless of the phase of  $\kappa$ . The condition on  $\kappa$  can be cast as a condition on the mass of the charged Higgs<sup>6</sup> and on  $\epsilon_2$ ,

$$\left(\frac{m_{H_{\pm}}^2 - m_W^2}{2v^2}\right)^2 > 3|\epsilon_2|^2 - 2\epsilon_{2r} \left(\frac{m_{H_{\pm}}^2 - m_W^2}{2v^2}\right) \quad (\text{condition for single minimum}) . \quad (\text{A4})$$

The condition (A4) depends on neither  $\tan\beta$  nor  $\epsilon_1$ . For  $|\epsilon_{2i,r}| \leq 0.1$ , it is fulfilled for  $m_{H_{\pm}} \gtrsim 170 \text{ GeV}$ . In case that  $\epsilon_{2r} > 0$ , it is enough to impose  $m_{H_{\pm}} > 130 \text{ GeV}$ . In fact, violation of Eq. (A4) necessarily implies  $m_{H_{\pm}}^2 \sim \epsilon_2 v^2$  [65]. This can be understood in general from the Georgi-Pais theorem [66]. (In our case, nonrenormalizable operators should be considered instead of quantum corrections to break the CP-symmetry of the potential.) Such low values for  $m_{H_{\pm}}$  (and hence also  $m_A$ ) are, in general, in tension with both direct and indirect experimental constraints. We did not pursue further the analysis of this parameter regime, even though it may have interesting consequences for EWBG via transitions between different phase vacua [67].

As a final comment, note that keeping the term of order  $\epsilon_2^2$  in Eq. (A4) is required for small  $m_{H_{\pm}}$ , where  $(m_{H_{\pm}}^2 - m_W^2)/2v^2$  becomes a small parameter  $\mathcal{O}(0.1)$ . As is the case in several points in this work, neglecting independent dimension six operators is still a consistent procedure.

## Appendix B: Quantum Corrections

Quantum corrections to the Higgs sector, in the presence of explicit CP violation in the MSSM, were discussed in detail in Refs. [24, 68] for zero temperature and Refs. [29, 30] for finite temperature. Here we present only the corrections that are directly relevant for the vev phase in the BMSSM. We consider squark, chargino, neutralino and scalar Higgs loops.

We write the potential as  $V = V_0 + \Delta V_1 + \Delta V_T$ , where  $V_0$  is the tree-level, zero-temperature part, given in Eq. (4),  $\Delta V_1$  is the zero-temperature one-loop part, and  $\Delta V_T$  is the finite-temperature correction. For  $\Delta V_1$ , one sums over all particle species with field dependent

---

<sup>6</sup> For  $\kappa$  on the real axis, the emergence of an additional solution with  $\theta \neq 0$  implies spontaneous CP violation. This situation was discussed in [64] for the BMSSM.



masses:

$$\Delta V_1 = \sum_i \frac{n_i m_i^4(\phi)}{64\pi^2} \left( \ln \frac{m_i^2(\phi)}{Q^2} - \frac{3}{2} \right), \quad (\text{B1})$$

where  $Q$  is the renormalization scale, which we choose as  $Q = m_t$ . For  $\Delta V_T$ , we include the pressure and daisy terms:

$$\Delta V_T = \sum_i \frac{n_i T^4}{2\pi^2} J \left( \frac{m_i^2(\phi)}{T^2} \right) - \sum_{i=\text{sca}} \frac{n_i T}{12\pi} [m_i^3(\phi, T) - m_i^3(\phi)], \quad (\text{B2})$$

where the second sum includes scalars and longitudinal gauge bosons and with the  $J$  functions defined by

$$J_{B,F}(x) = \int_0^\infty dy y^2 \ln \left( 1 \mp e^{-\sqrt{x+y^2}} \right). \quad (\text{B3})$$

Beginning with zero temperature, it is useful to first obtain an analytical estimate of the contributions from stops, charginos and neutralinos. We follow the procedure introduced in Section II, and apply it to  $V_0 + \Delta V_1$ . We find the corrected expressions for  $|b|$  and  $\theta$ ,

$$|b|^2 = \left[ \frac{s_{2\beta}}{2} (m_{H^\pm}^2 - m_W^2) + v^2 (s_{2\beta}\epsilon_{2r} - 2\epsilon_{1r}) - \text{Re} [e^{i\theta} \delta\mathcal{V}'] \right]^2 + \left[ v^2 (s_{2\beta}\epsilon_{2i} - 2\epsilon_{1i}) - \text{Im} [e^{i\theta} \delta\mathcal{V}'] \right]^2, \quad (\text{B4a})$$

$$\tan \theta = \frac{v^2 (s_{2\beta}\epsilon_{2i} - 2\epsilon_{1i}) - \text{Im} [e^{i\theta} \delta\mathcal{V}']}{\frac{s_{2\beta}}{2} (m_{H^\pm}^2 - m_W^2) + v^2 (s_{2\beta}\epsilon_{2r} - 2\epsilon_{1r}) - \text{Re} [e^{i\theta} \delta\mathcal{V}']}. \quad (\text{B4b})$$

The quantity  $\delta\mathcal{V}'(\propto \partial V/\partial\theta)$  encodes the various contributions:

$$\delta\mathcal{V}' \approx \delta_{\tilde{t}}\mathcal{V}' + \delta_{\tilde{C}}\mathcal{V}' + \delta_{\tilde{N}}\mathcal{V}', \quad (\text{B5})$$

where, to  $\mathcal{O}(\epsilon_1)$  and  $\mathcal{O}(g^2)$ , and neglecting contributions to the charged Higgs mass arising from diagrams involving chargino-neutralino and stop-sbottom loops, we have

$$\delta_{\tilde{t}}\mathcal{V}' \approx \frac{3y_t^2}{16\pi^2} \mathcal{G}(m_{\tilde{t}_2}, m_{\tilde{t}_1}) \left[ |A_t \mu| e^{i\phi_t} + 2v^2 |\epsilon_1| e^{i\vartheta_1} \left( c_\beta^2 - s_{2\beta} \left| \frac{A_t}{\mu} \right| e^{i(\phi_t + \theta)} \right) \right] \quad (\text{B6a})$$

$$\delta_{\tilde{C}}\mathcal{V}' \approx -\frac{|\epsilon_1 \mu^2| e^{i\vartheta_1}}{4\pi^2} \left( \ln \frac{|\mu|^2}{Q^2} - 1 \right) + \frac{g^2 |M_2 \mu| e^{i\phi_2}}{8\pi^2} \mathcal{G}(|M_2|, |\mu|) \quad (\text{B6b})$$

$$\delta_{\tilde{N}}\mathcal{V}' \approx -\frac{|\epsilon_1 \mu^2| e^{i\vartheta_1}}{4\pi^2} \left( \ln \frac{|\mu|^2}{Q^2} - 1 \right) + \frac{g^2 |M_2 \mu| e^{i\phi_2}}{16\pi^2} \mathcal{G}(|M_2|, |\mu|) + \frac{g'^2 |M_1 \mu| e^{i\phi_1}}{16\pi^2} \mathcal{G}(|M_1|, |\mu|). \quad (\text{B6c})$$

The loop function is

$$\mathcal{G}(m_a, m_b) = \frac{m_a^2 \ln \frac{m_a^2}{Q^2} - m_b^2 \ln \frac{m_b^2}{Q^2}}{m_a^2 - m_b^2} - 1. \quad (\text{B7})$$

The conditions that the CP violation induced by the usual MSSM loop corrections becomes comparable to the tree level nonrenormalizable contribution can be written as

$$\begin{aligned}\frac{\epsilon_1}{g^2/16\pi^2} &\lesssim \frac{3M_2\mu}{2v^2} \Leftrightarrow \frac{\epsilon_1}{0.05} \lesssim \frac{M_2\mu}{(600 \text{ GeV})^2}, \\ \frac{\epsilon_1}{y_t^2/16\pi^2} &\lesssim \frac{3A_t\mu}{2v^2} \Leftrightarrow \frac{\epsilon_1}{0.05} \lesssim \frac{A_t\mu}{(400 \text{ GeV})^2}.\end{aligned}$$

We learn that the BMSSM terms can easily dominate. Furthermore, if  $\phi_{1,2,t} \ll 1$ , the radiative corrections are unimportant as they mostly serve to slightly shift the value of  $|b|$ .

Eq. (B6) includes also a contribution from  $\epsilon_1$  itself, arising via its appearance in the squark and sfermion mass matrices. Here, the stop contribution is negligible compared to that of charginos and neutralinos. This reflects the fact that  $\epsilon_1$  corrects only the mass splitting of stops, while it enters the trace of higgsino mass matrices. The  $\epsilon_1$  loop correction tends to cancel the tree level term. It becomes relevant if  $\mu^2/v^2$  is large enough to compensate for the loop suppression; in practice, the term is significant for  $\mu \gtrsim 500 \text{ GeV}$ .

Finally, a common feature of the zero-T corrections of Eq. (B6) is that they depend only mildly on the vev. Hence, the net effect of these terms in the vicinity of the origin of field space is to globally shift the value of  $\theta$ . This implies that the phase variation across the bubble wall,  $\Delta\theta$ , and consequently the novel BMSSM contributions to the BAU, remain mostly unchanged.

Proceeding to finite temperature, let us again obtain some analytical understanding, beginning with the stop sector. We consider the plausible limit where the heavier stop,  $\tilde{t}_2$ , is Boltzmann suppressed, while the contribution of the lighter  $\tilde{t}_1$  admits a high-T expansion. Then,

$$\begin{aligned}b_{\text{eff}}(\phi, T) &\sim |b| + 2|\epsilon_1|\phi^2 e^{i\vartheta_1} + \frac{3y_t^2 T^2}{4m_{\tilde{t}_2}^2} (|A_t\mu|e^{i\phi_t} + 2|\epsilon_1|\phi^2 c_\beta^2 e^{i\vartheta_1}) \\ \epsilon_2(\phi, T) &\sim \epsilon_2 + \frac{3y_t^2 T^2}{2m_{\tilde{t}_2}^2} \frac{A_t\mu\epsilon_1}{|\mu|^2}.\end{aligned}\tag{B8}$$

While there is no loop suppression in Eq. (B8), the thermal correction at the critical temperature is still down by a factor  $\sim T_c^2/m_{Q_3}^2$ . Note also that the MSSM term  $\propto |A_t\mu|e^{i\phi_t}$  is field independent to  $\mathcal{O}(T_c^2\phi^2/m_{Q_3}^4)$ , such that its contribution to the variation of  $\theta$  across the bubble wall is suppressed. Using Eq. (B8), we can compare the tree level effect of the nonrenormalizable BMSSM terms with the leading thermal correction of the MSSM. Focusing

on the phase variation along the wall,

$$\left. \frac{\delta_{\text{BMSSM}}}{\delta_{\text{MSSM}}} \right|_{T>0} \sim 0.5 \left( \frac{\epsilon_1}{0.1} \right) \left( \frac{m_{Q_3}^2}{A_t \mu} \right) \left( \frac{T_c}{100 \text{ GeV}} \right)^{-2} \left( \frac{m_{Q_3}}{200 \text{ GeV}} \right)^2. \quad (\text{B9})$$

In the bulk of this paper, we isolate the novel BMSSM effects by using small or vanishing values of  $A_t$ , as well as vanishing  $\phi_t$ . Hence only the term proportional to  $\epsilon_1 \phi^2 c_\beta^2$  in Eq. (B8) remains. Since this term is field dependent, it does not affect the determination of  $\theta$  in the symmetric outskirts of the bubble wall, where  $\phi \ll T_c$ . Since it is doubly-tan  $\beta$  suppressed, it can typically be neglected with regard to the variation of  $\theta$  along the wall, even for  $m_{Q_3} \sim T_c$ .

Moving on to the Higgs and higgsinos, we find that Higgs-Higgs and Higgs-higgsino interactions lead to a non-negligible shift in the finite-temperature Higgs phase  $\theta(z)$  at  $\mathcal{O}(\epsilon_1)$ . This effect is easy to understand by considering a high temperature regime  $T > m$ , where  $m$  denotes any mass parameter in the Higgs and (weak) gaugino sectors. (Of course, at such high  $T > T_c$  the universe is globally symmetric. Nevertheless, it is illuminating to provisionally pursue this line of argument.) In this temperature regime and near the origin of field space, the one-loop thermal potential due to Higgs and higgsino particles can be expanded,

$$\begin{aligned} V_T^{\text{H},\tilde{\text{H}}} &\sim \frac{T^2}{24} \text{Tr} M_{H_0}^2 + \frac{T^2}{12} \text{Tr} M_{H_\pm}^2 + \frac{T^2}{24} \text{Tr} \mathbf{M}_{\tilde{N}}^\dagger \mathbf{M}_{\tilde{N}} + \frac{T^2}{12} \text{Tr} \mathbf{X}^\dagger \mathbf{X} \\ &\supset -\frac{3|\epsilon_1|T^2\phi^2 s_{2\beta}}{2} \cos(\theta + \vartheta_1), \end{aligned} \quad (\text{B10})$$

The phase-dependent piece of the potential becomes

$$V_T(\theta) \sim -\phi^2 s_{2\beta} \left[ |b| \cos \theta + 2|\epsilon_1| \left( \phi^2 + \frac{3T^2}{4} \right) \cos(\theta + \vartheta_1) - \frac{|\epsilon_2|\phi^2 s_{2\beta}}{2} \cos(2\theta + \vartheta_2) \right]. \quad (\text{B11})$$

In the high-T approximation and in the  $\cot \beta \gg |\epsilon_1|v^2/m_A^2$  regime, setting  $T = T_c$ , the values of  $\theta$  in the symmetric ( $s$ ) and broken ( $b$ ) phases are

$$\theta_s = \lim_{z \rightarrow -\infty} \theta(z) \sim -\arctan \frac{3|\epsilon_1|T_c^2 \sin \vartheta_1}{2|b| + 3|\epsilon_1|T_c^2 \cos \vartheta_1} \sim -\frac{3T_c^2 \epsilon_{1i}}{m_{H_\pm}^2 s_{2\beta}}, \quad (\text{B12})$$

$$\theta_b = \lim_{z \rightarrow +\infty} \theta(z) \sim \theta_s + \Delta\theta. \quad (\text{B13})$$

In other words, the dominant effect is to shift  $\theta(z)$  by  $\theta_s$  over the tree-level result [Eq. (27)]; however, the relative phase  $(\theta_b - \theta_s)$  that governs EWBG remains unchanged from its tree-level value of  $\Delta\theta$ .

We should make the following comment, regarding the calculation of  $\theta_s$  in Eq. (B12). Any dependence of the potential on  $\theta$  must be proportional to  $\phi^2 s_{2\beta}$ . Thus, in the truly

symmetric region where the vev vanishes, the value of  $\theta$  is not well defined. The quantity we denote by  $\theta_s$  corresponds to the value of the CP-violating phase in the almost symmetric regime, where the vev is finite, but smaller than any other mass scale in the problem. The non-zero value of  $\theta_s$  indicates that, in the complex plane, the origin can be approached from different directions. Since  $\theta$  cannot affect the dynamics in the symmetric regime, we may extend the definition of  $\theta_s$  to  $z \rightarrow -\infty$ . Having clarified this point, it is important to keep in mind that in the region of  $\phi < gT$  there are additional non-perturbative corrections to the scalar potential, which we do not consider here beyond the daisy resummation introduced in Eq. (B2). We note that the daisy corrections, which include  $\theta$ -dependent terms in the scalar self-energies, do not significantly affect our results for  $\theta_s$ .

In Fig. 6 we illustrate the role of quantum and thermal effects in dictating the complex vev phase at zero and finite temperature. We go beyond the approximation of Eqs. (B12) and (B13) by using the full one-loop thermal potential, instead of the high-T expansion given in Eq. (B10). We solve for the asymptotic values of the complex phase by minimizing the potential at the critical vev and near the origin of field space, setting  $T = T_c$ . Since the  $\epsilon_1$  loop contribution depends mainly on  $\mu$ , we use  $\mu$  as an independent variable. To emphasize the role of the T-dependent terms, we fix all parameters and repeat the plot in two panels, once for  $T_c = v_c = 100$  and once for  $T_c = 150$ ,  $v_c = 110$  GeV. We minimize the potential numerically, accounting also for the zero- and finite-temperature effects of the Higgs scalars. Two main features which were mentioned above are worth pointing out. First, the onset of the zero temperature effect appears at large  $\mu \sim 400$  GeV. Second, while quantum corrections shift  $\theta_s$  sizably, the value of  $\Delta\theta$ , the phase difference between the broken and symmetric domains, is much less affected.

## Acknowledgments

We thank J.R. Espinosa, T. Konstandin, D. Morrissey, A. Riotto and O. Vitells for helpful discussions. The work of Y.N. is supported by the Israel Science Foundation (ISF) under grant No. 377/07, by the German-Israeli foundation for scientific research and development (GIF), and by the United States-Israel Binational Science Foundation (BSF), Jerusalem,

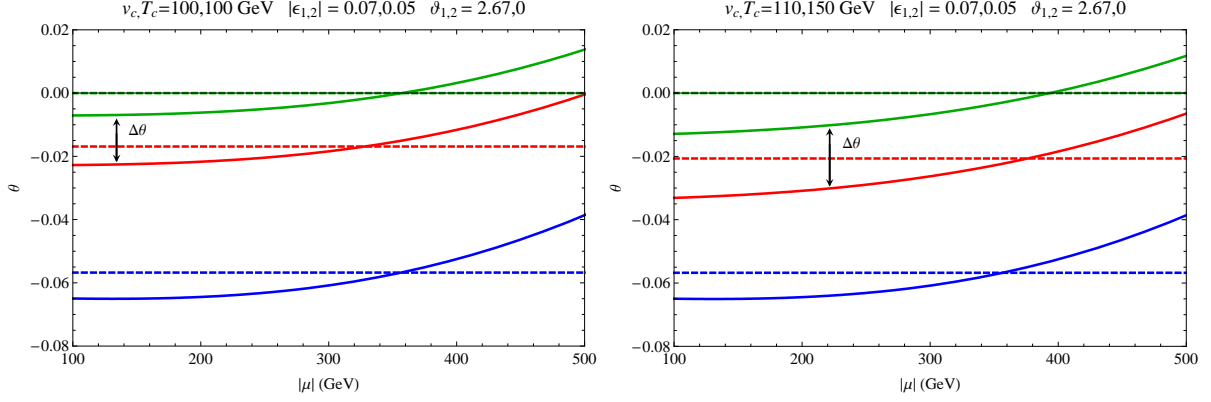


FIG. 6: The vev phase, including quantum and thermal corrections. Unspecified parameters are as in Table II. Left:  $T_c = 100$  GeV,  $v_c = 100$  GeV. Right:  $T_c = 150$  GeV,  $v_c = 110$  GeV. Green, red and blue curves correspond to  $\theta_s$ ,  $\theta_b = \theta_s + \Delta\theta$  and the zero- $T$  value of  $\theta$ , respectively. Dashed (solid) curves denote tree level (one loop) results.

Israel.

- 
- [1] A. D. Sakharov, Pisma Zh. Eksp. Teor. Fiz. **5**, 32 (1967) [JETP Lett. **5**, 24 (1967 SOPUA,34,392-393.1991 UFNAA,161,61-64.1991)].
  - [2] G. R. Farrar and M. E. Shaposhnikov, Phys. Rev. Lett. **70**, 2833 (1993) [Erratum-ibid. **71**, 210 (1993)] [arXiv:hep-ph/9305274]; Phys. Rev. D **50**, 774 (1994) [arXiv:hep-ph/9305275]; P. Huet and E. Sather, Phys. Rev. D **51**, 379 (1995) [arXiv:hep-ph/9404302]; M. B. Gavela, P. Hernandez, J. Orloff, O. Pene and C. Quimbay, Nucl. Phys. B **430**, 382 (1994) [arXiv:hep-ph/9406289].
  - [3] M. Drees and K. Hagiwara, Phys. Rev. D **42**, 1709 (1990).
  - [4] C. Amsler *et al.* [Particle Data Group], Phys. Lett. B **667** (2008) 1.
  - [5] M. Quiros, Nucl. Phys. Proc. Suppl. **101**, 401 (2001) [arXiv:hep-ph/0101230] and references therein.
  - [6] M. Carena, G. Nardini, M. Quiros and C. E. M. Wagner, Nucl. Phys. B **812**, 243 (2009) [arXiv:0809.3760 [hep-ph]].
  - [7] Y. Li, S. Profumo and M. Ramsey-Musolf, Phys. Lett. B **673**, 95 (2009) [arXiv:0811.1987 [hep-ph]].

- [8] V. Cirigliano, Y. Li, S. Profumo and M. J. Ramsey-Musolf, arXiv:0910.4589 [hep-ph].
- [9] M. Dine, N. Seiberg and S. Thomas, Phys. Rev. D **76**, 095004 (2007) [arXiv:0707.0005 [hep-ph]].
- [10] A. Brignole, J. A. Casas, J. R. Espinosa and I. Navarro, Nucl. Phys. B **666**, 105 (2003) [arXiv:hep-ph/0301121]; J. A. Casas, J. R. Espinosa and I. Hidalgo, JHEP **0401**, 008 (2004) [arXiv:hep-ph/0310137].
- [11] A. Strumia, Phys. Lett. B **466**, 107 (1999) [arXiv:hep-ph/9906266].
- [12] I. Antoniadis, E. Dudas, D. M. Ghilencea and P. Tziveloglou, Nucl. Phys. B **808**, 155 (2009) [arXiv:0806.3778 [hep-ph]].
- [13] P. Batra and E. Ponton, Phys. Rev. D **79**, 035001 (2009) [arXiv:0809.3453 [hep-ph]].
- [14] M. Pospelov, A. Ritz and Y. Santoso, Phys. Rev. D **74**, 075006 (2006) [arXiv:hep-ph/0608269].
- [15] K. Blum and Y. Nir, Phys. Rev. D **78**, 035005 (2008) [arXiv:0805.0097 [hep-ph]].
- [16] K. Cheung, S. Y. Choi and J. Song, Phys. Lett. B **677**, 54 (2009) [arXiv:0903.3175 [hep-ph]].
- [17] N. Bernal, K. Blum, Y. Nir and M. Losada, JHEP **0908**, 053 (2009) [arXiv:0906.4696 [hep-ph]].
- [18] M. Berg, J. Edsjo, P. Gondolo, E. Lundstrom and S. Sjors, JCAP **0908**, 035 (2009) [arXiv:0906.0583 [hep-ph]].
- [19] N. Bernal and A. Goudelis, JCAP **1003**, 007 (2010) [arXiv:0912.3905 [hep-ph]].
- [20] M. Carena, K. Kong, E. Ponton and J. Zurita, Phys. Rev. D **81**, 015001 (2010) [arXiv:0909.5434 [hep-ph]].
- [21] M. Pietroni, Nucl. Phys. B **402**, 27 (1993) [arXiv:hep-ph/9207227];
- [22] S. Dimopoulos and S. D. Thomas, Nucl. Phys. B **465**, 23 (1996) [arXiv:hep-ph/9510220].
- [23] S. P. Martin, arXiv:hep-ph/9709356.
- [24] S. Y. Choi, M. Drees and J. S. Lee, Phys. Lett. B **481**, 57 (2000) [arXiv:hep-ph/0002287].
- [25] S. W. Ham, S. a. Shim and S. K. OH, Eur. Phys. J. C **65**, 517 (2010) [arXiv:0909.5098 [hep-ph]].
- [26] K. Blum, C. Delaunay and Y. Hochberg, Phys. Rev. D **80**, 075004 (2009) [arXiv:0905.1701 [hep-ph]].
- [27] S. Schael *et al.* [LEP Collaboration], Eur. Phys. J. C **47**, 547 (2006) [arXiv:hep-ex/0602042]; P. Bechtle [LEP Collaboration], PoS **HEP2005**, 325 (2006) [arXiv:hep-ex/0602046].
- [28] M. S. Alam *et al.* [CLEO Collaboration], Phys. Rev. Lett. **74**, 2885 (1995).

- [29] D. Comelli and M. Pietroni, Phys. Lett. B **306**, 67 (1993) [arXiv:hep-ph/9302207]; K. Funakubo, A. Kakuto, S. Otsuki and F. Toyoda, Prog. Theor. Phys. **98**, 427 (1997) [arXiv:hep-ph/9704359]; M. Laine and K. Rummukainen, Nucl. Phys. B **545**, 141 (1999) [arXiv:hep-ph/9811369];
- [30] S. J. Huber, P. John, M. Laine and M. G. Schmidt, Phys. Lett. B **475**, 104 (2000) [arXiv:hep-ph/9912278].
- [31] M. E. Shaposhnikov, JETP Lett. **44** (1986) 465 [Pisma Zh. Eksp. Teor. Fiz. **44** (1986) 364].
- [32] M. S. Carena, M. Quiros and C. E. M. Wagner, Phys. Lett. B **380**, 81 (1996) [arXiv:hep-ph/9603420]; D. Delepine, J. M. Gerard, R. Gonzalez Felipe and J. Weyers, Phys. Lett. B **386**, 183 (1996) [arXiv:hep-ph/9604440];
- [33] D0 Collaboration, V. Abazov *et al.*, D0 Note 5931-CONF (2009).
- [34] J. M. Moreno, M. Quiros and M. Seco, Nucl. Phys. B **526**, 489 (1998) [arXiv:hep-ph/9801272].
- [35] S. J. Huber, P. John and M. G. Schmidt, Eur. Phys. J. C **20**, 695 (2001) [arXiv:hep-ph/0101249].
- [36] D. Comelli, M. Pietroni and A. Riotto, Phys. Rev. D **53**, 4668 (1996) [arXiv:hep-ph/9506278].
- [37] H. Kurki-Suonio and M. Laine, Phys. Rev. Lett. **77**, 3951 (1996) [arXiv:hep-ph/9607382].
- [38] A. Megevand, Phys. Rev. D **64**, 027303 (2001) [arXiv:hep-ph/0011019].
- [39] P. John, Phys. Lett. B **452**, 221 (1999) [arXiv:hep-ph/9810499].
- [40] A. Megevand and A. D. Sanchez, Nucl. Phys. B **825**, 151 (2010) [arXiv:0908.3663 [hep-ph]].
- [41] P. John and M. G. Schmidt, Nucl. Phys. B **598**, 291 (2001) [Erratum-ibid. B **648**, 449 (2003)] [arXiv:hep-ph/0002050]. G. D. Moore, JHEP **0003**, 006 (2000) [arXiv:hep-ph/0001274].
- [42] D. J. H. Chung, B. Garbrecht, M. J. Ramsey-Musolf and S. Tulin, arXiv:0905.4509 [hep-ph].
- [43] V. Cirigliano, M. J. Ramsey-Musolf, S. Tulin and C. Lee, Phys. Rev. D **73**, 115009 (2006) [arXiv:hep-ph/0603058].
- [44] D. J. H. Chung, B. Garbrecht, M. J. Ramsey-Musolf and S. Tulin, arXiv:0908.2187 [hep-ph].
- [45] A. Riotto, Phys. Rev. D **58**, 095009 (1998) [arXiv:hep-ph/9803357].
- [46] C. Lee, V. Cirigliano and M. J. Ramsey-Musolf, Phys. Rev. D **71**, 075010 (2005) [arXiv:hep-ph/0412354].
- [47] T. Prokopec, M. G. Schmidt and S. Weinstock, Annals Phys. **314**, 208 (2004) [arXiv:hep-ph/0312110]. Annals Phys. **314**, 267 (2004) [arXiv:hep-ph/0406140]. T. Konstandin, T. Prokopec and M. G. Schmidt, Nucl. Phys. B **716**, 373 (2005)

- [arXiv:hep-ph/0410135]. T. Konstandin, T. Prokopec, M. G. Schmidt and M. Seco, Nucl. Phys. B **738**, 1 (2006) [arXiv:hep-ph/0505103].
- [48] M. S. Carena, M. Quiros, M. Seco and C. E. M. Wagner, Nucl. Phys. B **650**, 24 (2003) [arXiv:hep-ph/0208043].
- [49] V. Cirigliano, C. Lee, M. J. Ramsey-Musolf and S. Tulin, arXiv:0912.3523 [hep-ph].
- [50] L. Fromme and S. J. Huber, JHEP **0703**, 049 (2007) [arXiv:hep-ph/0604159]. L. Fromme, S. J. Huber and M. Seniuch, JHEP **0611**, 038 (2006) [arXiv:hep-ph/0605242].
- [51] S. J. Huber, M. Pospelov and A. Ritz, Phys. Rev. D **75**, 036006 (2007) [arXiv:hep-ph/0610003].
- [52] J. Dunkley *et al.* [WMAP Collaboration], Astrophys. J. Suppl. **180** (2009) 306 [arXiv:0803.0586 [astro-ph]].
- [53] B. C. Regan, E. D. Commins, C. J. Schmidt and D. DeMille, Phys. Rev. Lett. **88**, 071805 (2002).
- [54] C. A. Baker *et al.*, Phys. Rev. Lett. **97**, 131801 (2006) [arXiv:hep-ex/0602020].
- [55] W. C. Griffith, M. D. Swallows, T. H. Loftus, M. V. Romalis, B. R. Heckel and E. N. Fortson, Phys. Rev. Lett. **102**, 101601 (2009).
- [56] M. Pospelov and A. Ritz, Annals Phys. **318**, 119 (2005) [arXiv:hep-ph/0504231].
- [57] S. Weinberg, Phys. Rev. Lett. **63**, 2333 (1989).
- [58] J. R. Ellis, J. S. Lee and A. Pilaftsis, JHEP **0810**, 049 (2008) [arXiv:0808.1819 [hep-ph]].
- [59] D. Chang, W. Y. Keung and A. Pilaftsis, Phys. Rev. Lett. **82**, 900 (1999) [Erratum-ibid. **83**, 3972 (1999)] [arXiv:hep-ph/9811202].
- [60] A. Pilaftsis, Phys. Lett. B **471**, 174 (1999) [arXiv:hep-ph/9909485]; Nucl. Phys. B **644**, 263 (2002) [arXiv:hep-ph/0207277].
- [61] Y. Li, S. Profumo and M. Ramsey-Musolf, Phys. Rev. D **78**, 075009 (2008) [arXiv:0806.2693 [hep-ph]].
- [62] M. Pospelov and A. Ritz, Phys. Rev. D **63**, 073015 (2001) [arXiv:hep-ph/0010037].
- [63] D. DeMille, *et al.*, Phys. Rev. A **61**, 052507 (2000); S. K. Lamoreaux and R. Golub, J. Phys. G **36**, 104002 (2009); B. E. Sauer, *et al.*, AIP Conf. Proc. **869**, 44 (2006); Y. K. Semertzidis *et al.* [EDM Collaboration], AIP Conf. Proc. **698**, 200 (2004).
- [64] S. W. Ham, S. A. Shim and S. K. Oh, Phys. Rev. D **80**, 055009 (2009) [arXiv:0907.3300 [hep-ph]].
- [65] A. Pomarol, Phys. Lett. B **287**, 331 (1992) [arXiv:hep-ph/9205247].



- [66] H. Georgi and A. Pais, Phys. Rev. D **10**, 1246 (1974).
- [67] D. Comelli, M. Pietroni and A. Riotto, Nucl. Phys. B **412**, 441 (1994) [arXiv:hep-ph/9304267].
- [68] A. Pilaftsis, Phys. Lett. B **435**, 88 (1998) [arXiv:hep-ph/9805373]; M. S. Carena, J. R. Ellis, A. Pilaftsis and C. E. M. Wagner, Nucl. Phys. B **586**, 92 (2000) [arXiv:hep-ph/0003180].